Local Approximation Based Material Averaging Approach in the Finite Integration Technique

Christoph Classen, Bastian Bandlow and Rolf Schuhmann
Fachgebiet Theoretische Elektrotechnik, Universität Paderborn
Warburger Straße 100, 33098 Paderborn, Germany
classen@tet.upb.de

Abstract — The a priori known field behavior in the vicinity of simple geometrical shapes is used to derive a new procedure for material averaging in the Finite Integration Technique. We investigate a two-dimensional setup so far. The accuracy of a staircase approximation of wave scattering at a dielectric cylinder is improved and the resulting errors are well below the common facet-weighted averaging procedures.

I. Introduction

The accuracy of simulation methods based on Yee-like Cartesian grids suffer from the staircasing effect. This effect occurs due to the approximations that have to be done when curved shapes are part of the computational domain. One possibility to avoid this effect is the use of conformal grids, like shown in e.g. [1], other possibilities to face this problem may be advanced material averaging methods. In this work we focus on an averaging procedure, which uses not only the material information but also the known field behavior in the vicinity of a simple geometrical shape. This idea is motivated by the usage of local basis functions in the flexible local approximation methods introduced by Tsukerman in [2]. Preliminary work has been done modifying the material matrices of the Finite Integration Technique (FIT) [3] in the vicinity of sharp edges [4].

In this contribution we show how to include a priori known analytic results locally into the material matrix for circular boundaries in a rectangular grid, in order to improve the overall accuracy. The modifications are only included in the direct vicinity of the curved object.

II. Finite Integration Technique

The FIT is based on a spatial segmentation of the computational domain by a dual-orthogonal grid pair, the primary grid G and the dual grid $\tilde{G}$. The degrees of freedom of the method are the so-called integral state variables, defined as integrals of the electric and magnetic field vectors over edges $L_i, \tilde{L}_i$ and facets $A_j, \tilde{A}_j$ of the primary grid G and the dual grid $\tilde{G}$, respectively:

$$\widehat{e}_i = \int_{L_i} \vec{E} \cdot d\vec{s} \qquad \widehat{\widehat{d}}_i = \int_{\tilde{A}_i} \vec{D} \cdot d\vec{A} \tag{1}$$

$$\widehat{\widehat{j}}_i = \int_{\tilde{A}_i} \vec{J} \cdot d\vec{A} \qquad \widehat{h}_j = \int_{\tilde{L}_j} \vec{H} \cdot d\vec{s} \qquad \widehat{\widehat{b}}_j = \int_{A_j} \vec{B} \cdot d\vec{A} \tag{2}$$

Using vector notation the Maxwell's grid equations can be written as

$$\mathbf{C}\widehat{\mathbf{e}} = -\frac{d}{dt}\widehat{\widehat{\mathbf{b}}} \qquad \tilde{\mathbf{C}}\widehat{\mathbf{h}} = \frac{d}{dt}\widehat{\widehat{\mathbf{d}}} + \widehat{\widehat{\mathbf{j}}} \tag{3}$$

with the material relations $\widehat{\widehat{\mathbf{d}}} = \mathbf{M}_\varepsilon \widehat{\mathbf{e}}$, $\widehat{\widehat{\mathbf{j}}} = \mathbf{M}_\kappa \widehat{\mathbf{e}}$ and $\widehat{\widehat{\mathbf{b}}} = \mathbf{M}_\mu \widehat{\mathbf{h}}$. The topological curl-operators $\mathbf{C}$ and $\tilde{\mathbf{C}}$ contain the entries {-1;0;1} only. The material matrices map the state variables from the primary to the dual grid, which causes the necessity to introduce some averaging at the material interfaces. For the permittivity matrix $\mathbf{M}_\varepsilon$ most commonly the facet based material averaging is used. We show an extended possibility: A field-based material averaging approach.

A. Facet-Based Material Averaging

The standard for the approximation of curved material boundaries is a staircase model and the facet-based averaging of permittivities. Up to four different permittivities are averaged by weighting them by the corresponding dual facets $\tilde{A}_j$ (see Fig. 1b).

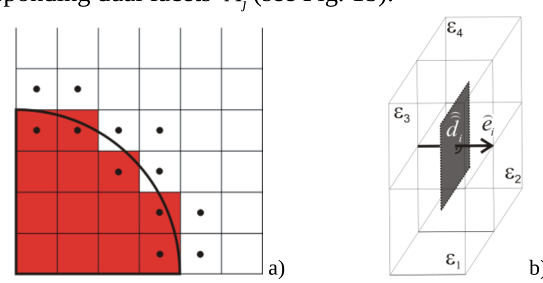

Fig. 1. a) Staircase effect, with a filling strategy based on the center of the mesh cells, allowing completely filled meshcells, only b) Facet-based material averaging of up to four different permittivities.

B. Field-Based Material Averaging

For the field-based averaging method we use the a priori available knowledge about the field behavior near specific geometrical shapes. In order to modify $\mathbf{M}_\varepsilon$ we can evaluate the integrals in (1) using this analytical knowledge of the fields and replace one entry in the permittivity matrix by the element-wise relation of $\widehat{\widehat{d}}_i$ and $\widehat{e}_i$. In the current implementation, we replace all those entries from the standard scheme (II.A.) where an averaging has taken place.

III. Computational Setup

Benchmark problems for convergence studies need a reliable reference for comparison reasons. Here, we calculate the scattering at a dielectric cylinder. The analytical solution is the sum of an incident plane wave expanded in cylindrical functions and the scattered field $E_z = E_z^i + E_z^s$ which reads outside the dielectric cylinder [5]

$$E_z = E_0 \sum_n \left(J_n(k_0\rho) + c_n H_n^{(2)}(k_0\rho) \right) j^{-n} e^{jn\phi} \quad \rho_0 < \rho \qquad (4)$$

with the relation $e^{-jx} = e^{-j\rho\cos\phi} = \sum_{n=-\infty}^{\infty} j^{-n} J_n(\rho) e^{jn\phi}$ and

$$E_{z,cyl} = E_0 \sum_n d_n J_n(k_{cyl}\rho) j^{-n} e^{jn\phi} \quad \rho \le \rho_0 \;. \qquad (5)$$

inside the cylinder. J_n and $H_n^{(2)}$ are Bessel and Hankel functions of second kind and order *n*. The radius of the cylinder is given by ρ_0 and the wave numbers k_{cyl} and k_0 are defined inside and outside the cylinder. The coefficients c_n and d_n are obtained by matching the continuity conditions resulting from Maxwell's equations. The analytical result of (4) and (5) is shown in Fig. 2 and Fig. 3a). In order to compare to the analytical results, we imprint the analytical solution as equivalent currents at the calculation domain boundaries. The curl-curl equation for the electric grid voltage $\widehat{\mathbf{e}}$ and the exciting currents $\widehat{\widehat{\mathbf{j}}}$ reads

$$\left(\tilde{\mathbf{C}} \mathbf{M}_\mu^{-1} \mathbf{C} - \omega^2 \mathbf{M}_\varepsilon \right) \widehat{\mathbf{e}} = -j\omega \widehat{\widehat{\mathbf{j}}} \,, \qquad (6)$$

where the discrete grid current $\widehat{\widehat{\mathbf{j}}}$ on the right hand side include these equivalent currents as derived from the analytical solution (4) at the boundaries.

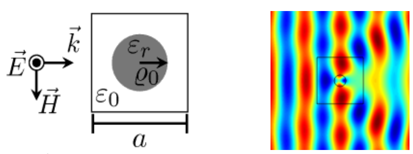

Fig. 2. Setup of wave scattering at a dielectric cylinder and resulting analytical solution from [5]. The black lines mark the final calculation domain.

IV. Numerical Results

The numerical setup and the polarization and the direction of the exciting plane wave is given in Fig. 2. As dimensions we choose $a = 1\text{m}$, $\rho_0 = \frac{a}{4}$, $\varepsilon_r = 11.56$ and $k_0 = \frac{4}{a}\text{m}^{-1}$.

We solve (6) using laboratory codes in Matlab. As a first test, the field behavior used for the modified entries in $\mathbf{M}_\varepsilon$ is assumed to be proportional to a mode of azimuthally zeroth order (see Fig. 3b), which results from neglecting the $J_n(k_0\rho)$ term of the incident wave in (4) and reducing the sum to the $n = 0$ term. The integration of the electric grid flux in (1) over a dual grid facet is done numerically.

Fig. 4 shows the convergence behavior (maximum norm of the deviation of the electric field) for different mesh and averaging types. For the analytical result *n*=60 azimuthal orders are superposed. The parameter *h* is the step width of the equidistant Cartesian grid. The standard convergence behavior is obtained by a staircase approximation, in which no partially filled meshcells occur. The simulations using the modified permittivity coefficients based on the analytical field behavior show a reduced overall error.

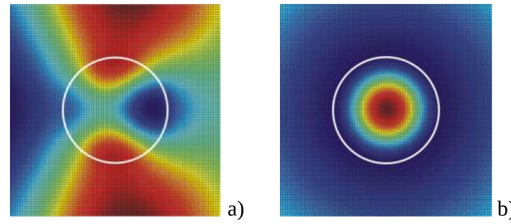

Fig. 3. a) Complete analytic solution E_z in the vicinity of the cylinder. b) The azimuthally zeroth order mode in E_z only is used for the field-based averaging approach.

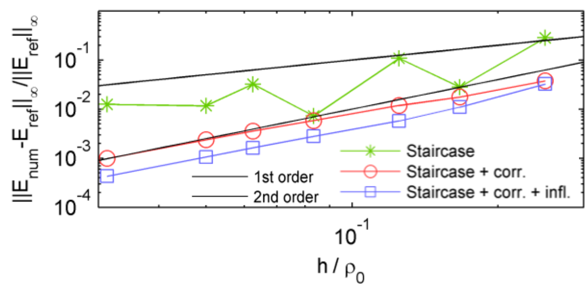

Fig. 4. Convergence behavior for different setups. The staircase results (*) are shown for reference. The new introduced correction by the field-based material averaging reduces the absolute error (O). Introducing an influence band $\rho_0 \pm \rho_0 / 4$ reduces the error even more (□).

V. Conclusions

The potential of accuracy enhancement of field-based material averaging at the boundaries of simple geometrical shapes has been investigated. A priori available knowledge about the field distribution in the vicinity of simple geometrical shapes is taken into account to derive modified permittivity matrices. The absolute error in the convergence curve of staircase approximations is reduced by using this kind of material averaging.

Following an idea introduced in [4], the modifications of the permittivity matrix are not limited to direct with the cylinder boundaries linked meshcells. It is possible to change a few matrix entries in a band of influence in the vicinity of the cylinder. First results of this approach look very promising for a further reduction of the error. In a similar manner, higher order basis functions may be applied for the correction.

VI. References

[1] R. Schuhmann, T. Weiland, "Stability of the FDTD Algorithm on Nonorthogonal Grids Related to the Spatial Interpolation Scheme" *IEEE Transactions on Magnetics*, vol. 34,5, pp. 2751-2754, 1998.

[2] I. Tsukerman, "Electromagnetic applications of a new finite-difference calculus", *Magnetics, IEEE Transactions on*, vol. 41, no. 7, pp. 2206–2225, July 2005.

[3] T. Weiland, "Eine Methode zur Lösung der Maxwellschen Gleichungen für sechskomponentige Felder auf diskreter Basis", *Archiv für Elektronik und Übertragungstechnik*, vol. 31, pp. 116-120, 1977.

[4] C. Classen, B. Bandlow, R. Schuhmann and I. Tsukerman, "FIT & FLAME for Sharp Edges in Electrostatics," *International URSI Symposium on Electromagnetic Theory EMTS 2010 - Symposium Digest*, 16. - 19. August Berlin, Germany, pp. 56-59, 2010.

[5] R. F. Harrington, "Time-Harmonic Electromagnetic Fields", McGraw-Hill Book Company, New York, 1961.